

Surface roughness and adsorption isotherms of molecularly thin liquid films: An x-ray reflectivity study

M. Paulus, C. Gutt,* and M. Tolan

Institute of Physics, University of Dortmund, 44221 Dortmund, Germany

(Received 26 July 2005; published 6 December 2005)

We present an x-ray reflectivity study of molecularly thin films of liquid isobutane adsorbed on liquid glycerol. The glycerol-isobutane interface serves as a model system to investigate the influence of the substrate adsorbate interactions on both adsorption isotherms and capillary wave fluctuations. The measured surface roughness is smaller than expected from the harmonic approximation of the interaction potential. Expressions for the surface roughness in slightly anharmonic potentials are given and compared to the experimental data. A good agreement between data and theory is achieved.

DOI: [10.1103/PhysRevE.72.061601](https://doi.org/10.1103/PhysRevE.72.061601)

PACS number(s): 68.03.-g, 68.15.+e, 61.10.-i

I. INTRODUCTION

Liquid-gas interfaces are very common in nature and in many technical applications. A large number of physical and chemical processes take place at this interface, e.g., the solution of gas molecules in the liquid, adsorption of gas molecules on the liquid surface, and catalytic reactions.

The interaction between the liquid surface and the gas molecules is usually dominated by long-ranging van der Waals forces. This interaction gives rise to adsorption of gas molecules on the liquid surface. At higher gas densities thin layers of adsorbed gas cover the surface.

Liquid surfaces are subject to thermally excited capillary wave fluctuations which give rise to a surface roughness of the order of a few angstroms. In the case of thin adsorbed films these fluctuations are reduced in their amplitude due to the interaction with the substrate leading to a thickness dependent surface roughness, which has already been observed in x-ray reflectivity experiments [1]. The most simple ansatz to describe the capillary wave roughness of an adsorbed thin liquid film is based on a harmonic approximation of the interfacial potential around its equilibrium thickness. While this approach gave reasonable results for the surface roughness of thick films (i.e., film thickness $d > 80$ Å) [2–4] it is also known that for lower film thicknesses the harmonic approximation fails to describe the measured surface roughnesses [3].

Several attempts have been made to obtain theoretical expressions for the surface roughness of thin liquid films in more realistic anharmonic potentials. Heilmann *et al.* [1] published a self-consistent formalism for interfacial fluctuations in potentials containing only even ($2n$) potential terms. Mecke [5] developed a self-consistent formalism to describe the surface roughness of liquid films on solid substrates in arbitrary potentials. This method has also been applied to the surface roughness of fluctuating bilayers [6]. Recently Li *et al.* [7] applied the method of functional integration to the theoretical problem of correlations between coupled liquid-

liquid surfaces. This method is based on a Taylor expansion of the interaction potential around the equilibrium film thickness. Li *et al.* calculated correlation functions by including the third-order term in the interfacial potential. It turns out that this method is especially well suited for our purpose and we extend their calculation to include terms of fourth order in the potential. We obtain analytical expressions for the film thickness and surface roughness including higher order potential terms.

The adsorption of gas molecules on solid substrates is a very well studied phenomenon. The standard characterization of thin adsorbed films is based on measurements of adsorption isotherms, which yields the film thickness as a function of gas pressure. Usually adsorption isotherms are described within the framework of the FHH (Frenkel-Halsey-Hill) theory based on van der Waals forces [8–10]. Deviations from the FHH theory have been assigned to thermal fluctuations of the interfacial profile of the thin liquid film [11,12].

It becomes clear that a more complete picture of surface adsorption requires the measurement of both adsorption isotherm and surface roughness. In this paper we present the first experiment that measures simultaneously film thickness, electron density, and surface roughness by means of x-ray reflectivity under isothermal conditions. From the experiment we obtain both the adsorption isotherm and the film thickness dependent surface roughness. For this purpose we choose a model system of liquid glycerol as substrate and isobutane as adsorbent. The use of a liquid substrate has the advantage of a well defined homogenous and flat substrate of well known (capillary wave) surface roughness. Isobutane is a relatively small molecule and provides a good electron density contrast to glycerol. In addition, it has an experimentally favorable low condensation pressure.

The paper is organized as follows: In Sec. II we first describe the theoretical background for x-ray scattering experiments and the theoretical predictions for the liquid surface roughness based on the approach using functional integration. Section III contains experimental setup and measurement technique. Experimental results and the discussion are presented in Sec. IV. Our findings are summarized in Sec. V. In an Appendix, we present details of the calculations.

*Present address: Deutsches Elektronen Synchrotron (HASYLAB), Notkestraße 85, D22607 Hamburg, Germany.

II. THEORY

A. X-ray scattering from thin liquid films

In x-ray reflectivity experiments the (vertical) electron density profile of the sample is probed by measuring the scattered radiation under specular condition. The wave-vector transfer has only one component perpendicular to the surface given by $q_z = (4\pi/\lambda)\sin\alpha$, where λ denotes the wavelength of the radiation and α denotes the angle between the surface and the x-ray beam.

The x-ray reflectivity data is analyzed with a simple model of a one-dimensional electron density profile. The profile consists of a substrate and a layer with electron densities ρ_1 and ρ_2 and Gaussian roughness parameters $\sigma_{1\text{eff}}$ and $\sigma_{2\text{eff}}$, respectively. In order to compare the roughness parameters $\sigma_{1\text{eff}}$ and $\sigma_{2\text{eff}}$ from our model with theoretical expressions based on capillary wave theory the scattering function has to be calculated.

We assume that the electron density ρ of a liquid-liquid interface that is subject to capillary wave fluctuations can be approximated by the following expression

$$\rho(x, y, z) = \Delta\rho_1 H(z - z_1(x, y)) + \Delta\rho_2 H(z - z_2(x, y)), \quad (1)$$

where $\Delta\rho_1$ denotes the difference in electron densities between glycerol and isobutane and $\Delta\rho_2$ the electron density difference between isobutane and its vapor phase, respectively. The liquid-adsorbate interface is located at $z_1(x, y)$ and the adsorbate-vapor interface at $z_2(x, y)$. $H(z)$ denotes the Heaviside function. Assuming that the capillary wave fluctuations are Gaussian random variables, the following scattering function at the specular position is obtained within the first Born approximation

$$S(q_z) = \frac{1}{q_z^2} \left(\sum_{i=1}^2 \Delta\rho_i^2 e^{-q_z^2 \sigma_i^2} \int dXdY e^{q_z^2 C_{ii}(X, Y)} R(X, Y) + 2\Delta\rho_1 \Delta\rho_2 \cos(q_z l_m) e^{-(1/2)q_z^2 (\sigma_1^2 + \sigma_2^2)} \times \int dXdY e^{q_z^2 C_{12}(X, Y)} R(X, Y) \right), \quad (2)$$

where $C_{ij}(X, Y) = \langle z_i(0, 0) z_j(X, Y) \rangle$ denotes the height-height and cross correlation functions of the system and l_m the thickness of the adsorbed film. Equation (2) has been intensively discussed by Heilmann *et al.* [1]. The surface roughness is defined via $\sigma_i^2 = C_{ii}(0, 0)$ in real space or via $\sigma_i^2 = (A/4\pi^2) \int_{q_{\text{grav}}}^{q_{\text{uc}}} d\mathbf{q} \langle \tilde{z}_i(\mathbf{q}) \tilde{z}_i(-\mathbf{q}) \rangle$ in Fourier space. The lower cutoff is given by gravity $q_{\text{grav}} = \sqrt{\rho_m g / \gamma} \sim 10^{-7} \text{ \AA}^{-1}$ with the mass density ρ_m , surface tension γ , and acceleration due to gravity g . The upper cutoff is usually assumed to be $q_{\text{up}} \approx \pi/r_M = 1 \text{ \AA}^{-1}$ with r_M approximating the size of the molecule. A is a unit area. $R(X, Y)$ is a real space cutoff function accounting for the finite coherence length of the x-ray beam on the sample [13]. In Fourier space the finite coherence length leads to a maximum observable capillary wave vector of $q_{\text{res}} = \pi/\xi_c$ where ξ_c is the projected coherence length of the x-ray beam on the liquid surface. Due to the long-range correlation of capillary waves, resolution effects are very important and affect the measured surface roughness consider-

ably [14,15]. The substrate-adsorbate interaction suppresses capillary waves on the adsorbed film larger than a specific van der Waals cutoff given by $q_{\text{vdW}}^2 = A_{\text{eff}} / (2\pi\gamma l_m^4)$, with A_{eff} denoting the effective Hamaker constant. For our system we find three well separated length scales as $q_{\text{vdW}} \gg q_{\text{res}} \gg q_{\text{grav}}$, which simplifies the situation considerably since we can approximate Eq. (2) by

$$S(q_z) \approx \frac{1}{q_z^2} \left(\sum_{i=1}^2 \Delta\rho_i^2 e^{-q_z^2 \sigma_{i\text{eff}}^2} + 2\Delta\rho_1 \Delta\rho_2 \cos(q_z l_m) e^{-(1/2)q_z^2 (\sigma_{1\text{eff}}^2 + \sigma_{2\text{eff}}^2)} \right), \quad (3)$$

with an effective surface roughness $\sigma_{i\text{eff}}^2 = (A/4\pi^2) \int_{q_{\text{res}}}^{q_{\text{uc}}} d\mathbf{q} \langle \tilde{z}_i(\mathbf{q}) \tilde{z}_i(-\mathbf{q}) \rangle$. Thus, including the resolution function into the scattering function leads to a replacement of the gravitational cutoff by the much larger resolution cutoff.

B. Determination of the surface roughness

Our system consists of a liquid substrate with a very low vapor pressure and interfacial tension γ_1 . On top of the substrate is a liquid film of thickness l and surface tension γ_2 . The adsorbed film is in equilibrium with its vapor phase at pressure p and the interaction between the substrate and the film can be described by an effective Hamaker constant A_{eff} . Then the free energy per unit area reads

$$F(l) = \gamma_1 + \gamma_2 + \Delta G, \quad (4)$$

with the interfacial potential

$$\Delta G = -\frac{A_{\text{eff}}}{12\pi l^2} + l\Delta\rho k_B T \ln(p_0/p), \quad (5)$$

where p_0 denotes the condensation pressure of the gas and $\Delta\rho$ the particle density difference between the adsorbed liquid and the vapor phase. A stable film requires a minimum of the free energy, which is given by

$$l_m = \left(\frac{A_{\text{eff}}}{6\pi\Delta\rho k_B T \ln(p/p_0)} \right)^{1/3}. \quad (6)$$

1. The harmonic approximation

In the harmonic approximation the potential is expanded to second order around its minimum position l_m . This leads to the free energy of the system [16]

$$F = \frac{1}{A} \int d^2r \left(\gamma_1 \left(1 + \frac{1}{2} |\nabla \xi_1|^2 \right) + \gamma_2 \left(1 + \frac{1}{2} |\nabla \xi_2|^2 \right) + \frac{1}{2} \frac{\partial^2 \Delta G}{\partial l^2} \Big|_{l_m} (\xi_1 - \xi_2)^2 \right). \quad (7)$$

$\xi_i(\mathbf{r})$ describes the deviation of the interface i from its mean position. Inserting the Fourier transforms $\xi_i(\mathbf{r}) = \sum_{\mathbf{q}} \tilde{\xi}_i(\mathbf{q}) \exp(i\mathbf{q}\mathbf{r})$ of the height-height fluctuations into the free energy, one obtains the canonical averages

$\langle \tilde{\xi}_i(\mathbf{q}) \tilde{\xi}_j(-\mathbf{q}) \rangle$ which are given, e.g., in [16,17].

The width of the substrate-film interface is obtained via $\sigma_1^2 = (A/4\pi^2) \int_{q_{lc}}^{q_{uc}} d\mathbf{q} \langle \tilde{\xi}_1(\mathbf{q}) \tilde{\xi}_1(-\mathbf{q}) \rangle$ which is

$$\sigma_1^2 = \frac{k_B T}{4\pi\gamma_1} \left(\frac{\gamma_1}{\gamma_1 + \gamma_2} \ln \left(\frac{q_{uc}^2(\kappa + q_{lc}^2)}{q_{lc}^2(\kappa + q_{uc}^2)} \right) + \ln \left(\frac{\kappa + q_{uc}^2}{\kappa + q_{lc}^2} \right) \right) \quad (8)$$

with $\kappa = [B(\gamma_1 + \gamma_2)]/\gamma_1\gamma_2$, $B = (\partial^2 \Delta G / \partial l^2)|_{l_m}$ and the lower wave-vector cutoff q_{lc} . This value is determined by the resolution of the diffractometer via $q_{lc} = q_z \Delta\alpha/2$, where $\Delta\alpha$ is the measured angular acceptance of the detector [15,18]. Similarly, we obtain the interfacial width of the liquid film as

$$\sigma_2^2 = \frac{k_B T}{4\pi\gamma_2} \left(\frac{\gamma_2}{\gamma_1 + \gamma_2} \ln \left(\frac{q_{uc}^2(\kappa + q_{lc}^2)}{q_{lc}^2(\kappa + q_{uc}^2)} \right) + \ln \left(\frac{\kappa + q_{uc}^2}{\kappa + q_{lc}^2} \right) \right). \quad (9)$$

A calculation of the surface roughnesses σ_1 according to Eq. (8), using the literature values of the surface tension of liquid glycerol and liquid isobutane and an effective Hamaker constant $A_{\text{eff}} = -8 \cdot 10^{-20}$ J, shows that the roughness σ_1 of the liquid substrate is not affected by the adsorbed thin film. This is due to the very different surface tensions of the two liquids, i.e., $\gamma_1 \gg \gamma_2$. This means that with regards to the surface roughness the liquid substrate behaves almost like a solid substrate. Based on this and on numerical calculations we find that we can rewrite the canonical averages for our purposes as follows:

$$\langle \tilde{\xi}_1(\mathbf{q}) \tilde{\xi}_1(-\mathbf{q}) \rangle = \frac{k_B T}{A} \frac{1}{\gamma_1 q^2}, \quad (10)$$

$$\langle \tilde{\xi}_2(\mathbf{q}) \tilde{\xi}_2(-\mathbf{q}) \rangle = \langle \tilde{u}_2(\mathbf{q}) \tilde{u}_2(-\mathbf{q}) \rangle + \chi(q)^2 \langle \tilde{\xi}_1(\mathbf{q}) \tilde{\xi}_1(-\mathbf{q}) \rangle, \quad (11)$$

$$\langle \tilde{\xi}_1(\mathbf{q}) \tilde{\xi}_2(-\mathbf{q}) \rangle = \chi(q) \langle \tilde{\xi}_1(\mathbf{q}) \tilde{\xi}_1(-\mathbf{q}) \rangle \quad (12)$$

with the replication factor $\chi(q) = \beta^2 / (\beta^2 + q^2 l_m^4)$, $\beta^2 = A_{\text{eff}} / (2\pi\gamma_2)$ [19] and

$$\langle \tilde{u}_2(\mathbf{q}) \tilde{u}_2(-\mathbf{q}) \rangle = (1 - \chi(q)) \frac{k_B T}{A} \frac{1}{\gamma_2 q^2}. \quad (13)$$

2. The anharmonic approximation

In the following, we assume that u_2 and ξ_1 are statistically independent. For the anharmonic approximation we consider the fluctuations of the film-vapor interface only. The term ΔG is expanded to 4th order around its minimum position leading to the free energy of the system

$$F = \frac{1}{A} \int d^2 r \left(\gamma_2 + \frac{\gamma_2}{2} (\nabla u_2)^2 + \frac{B}{2} u_2^2 + \frac{C}{6} u_2^3 + \frac{D}{24} u_2^4 \right) \quad (14)$$

with $C = (\partial^3 \Delta G / \partial l^3)|_{l_m}$ and $D = (\partial^4 \Delta G / \partial l^4)|_{l_m}$. We are using the technique of functional integration to calculate correla-

tion functions by treating the anharmonic terms u_2^3 and u_2^4 perturbatively. Details of the calculation can be found in the Appendix.

As has been noted by Li *et al.* [7] the presence of the third-order term C in the potential leads to a nonzero expectation value $\langle u_2 \rangle$. Using the potential form given in Eq. (5) we find the film thickness to increase proportional to the capillary wave fluctuations

$$\langle l \rangle = l_m + \frac{2}{l_m} \left(\frac{k_B T}{4\pi\gamma_2} \ln \left(\frac{B/\gamma_2 + q_{uc}^2}{B/\gamma_2} \right) \right), \quad (15)$$

The fourth-order term D decreases the mean square fluctuation of u_2 , and we find the following expression

$$\langle u_2(0) u_2(0) \rangle = \frac{k_B T}{4\pi\gamma_2} \ln \left(\frac{B/\gamma_2 + q_{uc}^2}{B/\gamma_2} \right) \left(1 - D \frac{k_B T}{4\pi} \left(\frac{1}{\gamma_2 B} - \frac{1}{\gamma_2 B + q_{uc}^2} \right) \right). \quad (16)$$

Based on the observation that the roughness σ_1 is hardly affected by the adsorbed film, we write for the Fourier components of ξ_2

$$\tilde{\xi}_2(\mathbf{q}) = \tilde{u}_2(\mathbf{q}) + \chi(q) \tilde{\xi}_1(\mathbf{q}). \quad (17)$$

The final result for the surface roughness of the thin liquid film is obtained by calculating

$$\sigma_2^2 = \frac{A}{4\pi^2} \int_{q_{lc}}^{q_{uc}} d\mathbf{q} \langle \tilde{\xi}_2(\mathbf{q}) \tilde{\xi}_2(-\mathbf{q}) \rangle$$

using that u_2 and ξ_1 are statistically independent leads to [20]

$$\sigma_2^2 = \langle u_2(0) u_2(0) \rangle + \frac{A}{4\pi^2} \int_{q_{lc}}^{q_{uc}} d\mathbf{q} \chi(q)^2 \langle \tilde{\xi}_1(\mathbf{q}) \tilde{\xi}_1(-\mathbf{q}) \rangle. \quad (18)$$

III. EXPERIMENT

The x-ray measurements were performed with a Bruker D8-Advanced diffractometer in theta-theta geometry. The x-ray radiation is produced by an x-ray tube with copper anode and focused by a Goebel mirror yielding a parallel x-ray beam of wavelength $\lambda = 1.54$ Å. A vertical slit of size 0.1 mm and a horizontal slit of size 10 mm were used to define the beam size on the sample. The scattered radiation is detected by a scintillation detector. The angular resolution $\Delta\alpha_f$ calculated from the detector slit setting was $\Delta\alpha_f \approx 0.4$ mrad. A typical x-ray reflectivity has been recorded within 2 to 3 hours.

The sample cell used is based on a design described in Ref. [21]. This sample cell was especially designed to measure x-ray reflectivities with a high temperature and a high pressure stability. The cell has a two-chamber design, where the outer chamber, which can be evacuated, is indispensable for thermal isolation. The inner cell can be pressurized up to a pressure of approximately 5 bar. The liquid sample is placed on a stainless steel plate with a diameter of 120 mm.

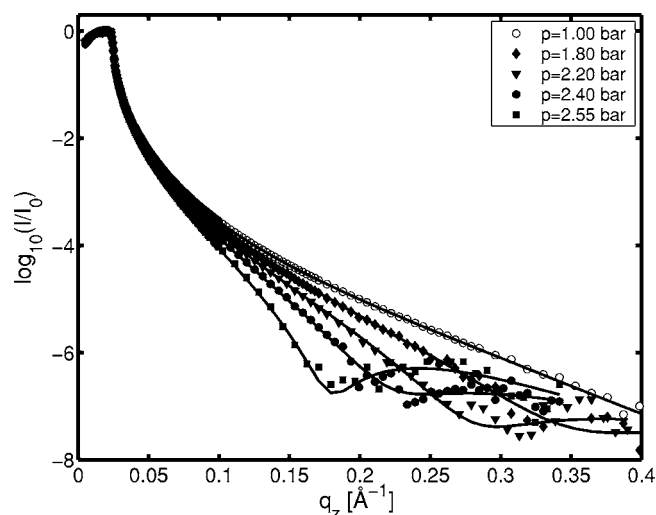


FIG. 1. X-ray reflectivity data (symbols) of the system isobutane/glycerol for different gas pressures and refinements (lines) with a single layer model.

The depth of the liquid sample is around 2 mm. Two thermal sensors (Pt100 elements) monitor the temperature of the gas and the liquid. The inner cell is mounted on a heat exchanger which stabilizes the sample temperature on a given value with a stability of 50 mK via a Lakeshore control unit. The pressure is monitored by a pressure gauge with a resolution of 1 mbar. The pressure stability was around 20 mbar during a typical reflectivity scan.

Both cells have thin (50 μm) Kapton windows for the incoming and reflected x-ray beam. For all measurements liquid glycerol ($\text{C}_3\text{H}_8\text{O}_3$) from Merck (purity >99%) and Isobutane 2.5 (C_4H_{10}) (Messer Griessheim) were used. All reflectivity measurements were performed at a film temperature of 15.8 $^\circ\text{C}$. After filling the glycerol into the sample plate the inner sample cell was filled with nitrogen gas of 1 bar pressure and an x-ray reflectivity of the nitrogen-glycerol interface was measured. At this condition the amount of adsorbed nitrogen is negligible and the N_2 -glycerol interface serves as a calibration system for an empty liquid substrate.

Before taking reflectivities of the isobutane-glycerol interface the inner cell was flushed for several minutes with isobutane. After this, x-ray reflectivities were measured at different pressures between 1.0 and 2.6 bar, which is close to the condensation pressure $p_0=2.66$ bar of isobutane at 15.8 $^\circ\text{C}$. Reflectivities at a single pressure value have been measured 3–6 times in order to exclude any systematical fluctuations to influence the results.

Finally, the inner cell was refilled with nitrogen and a control reflectivity of the nitrogen glycerol interface was performed.

IV. EXPERIMENTAL RESULTS AND DISCUSSION

Figure 1 shows x-ray reflectivities measured at different gas pressures. At low gas pressure the reflectivity curve is typical for a single surface with capillary wave roughness.

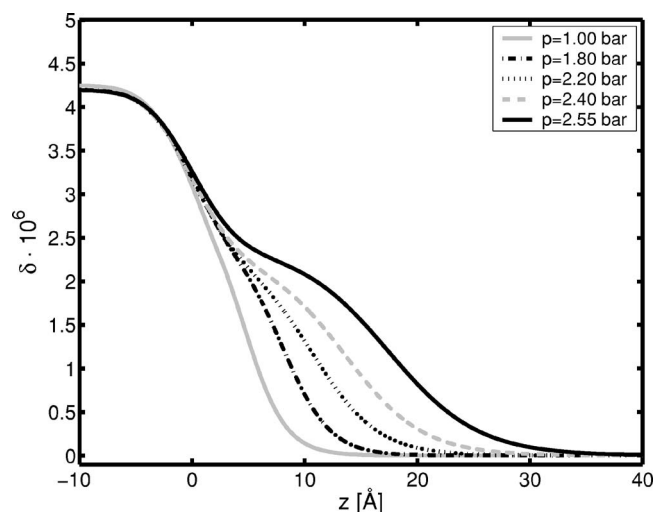


FIG. 2. The dispersion profiles for different isobutane pressures as extracted from the x-ray reflectivity measurements shown in Fig. 1. The dispersion is proportional to the electron density ρ_e according to $\delta=r_e\rho_e\lambda^2/(2\pi)$ with r_e denoting the classical electron radius.

Our refinement of the reflectivity of the empty glycerol surface yields a capillary wave roughness of the substrate of $\sigma_1=3.2$ \AA . This is in good agreement with standard capillary wave theory [22]. With increasing gas pressure a Kiessig fringe appears that indicates the presence of a layer with an electron density different from the underlying substrate. The maximum observed layer thickness was $l=23$ \AA .

At a laboratory x-ray source the maximum value of the wave-vector transfer is limited. Thus, we cannot expect to reveal small details of the electron density profile, especially for the very thin films. This requires the number of fit parameters to be as small as possible. Our adsorbed films provide film thicknesses that are comparable with the roughness, and it is well known that the usual Paratt algorithm fails for such electron density profiles. Therefore we used the model of an effective electron density for the final refinement of our data [4] where the electron density profile is split into very thin slices. For the thickest film we used four parameters to model the electron density profile: the interfacial width σ_1 between glycerol and isobutane, the electron density ρ of the adsorbed layer, its thickness l , and the surface roughness σ_2 of the layer. The refinements yield values of σ_1 similar to that of the empty substrate, which is consistent with the expression in Eq. (8). The electron density of the adsorbed layer was found to be equal to the value of bulk liquid isobutane. Thus we kept those two parameters constant for all refinements of the thinner films. Therefore, only the layer thickness and the surface roughness of the adsorbed film were refined. Figure 2 shows the resulting electron density profiles as obtained from the data analysis. The increasing adsorption of gas molecules on the substrate is clearly visible.

The resulting film thickness as a function of the relative gas pressure p/p_0 yields the adsorption isotherm that is displayed in Fig. 3. The solid line represents a refinement of Eq. (6) to the data leading to an effective Hamaker constant of $A_{\text{eff}}=-9 \times 10^{-20}$ J. Figure 4 shows the surface roughness σ_2

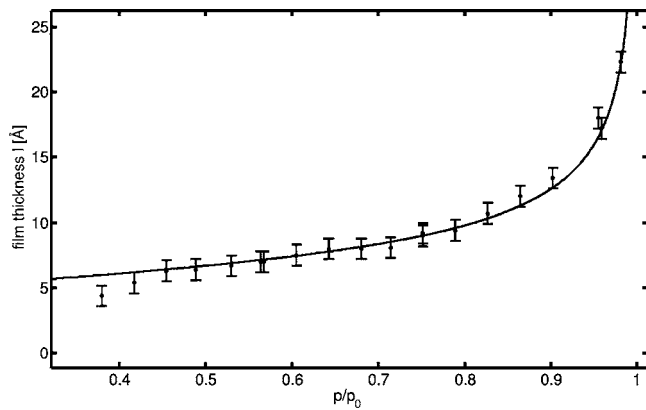


FIG. 3. Adsorption isotherm obtained from the x-ray reflectivity measurements. The solid line is a calculation of the film thickness l as a function of the normalized pressure p/p_0 according to Eq. (6).

of the adsorbed film as a function of the film thickness. Up to a film thickness of 8 to 9 Å the surface roughness is found to be constant at the value of the surface roughness of the underlying substrate (dashed line). After this it starts to increase to a maximum value for the thickest film of $\sigma_2 = 8$ Å. The dashed-dotted line represents a refinement with the harmonic approximation according to Eq. (9). The best fit has been obtained with a surface tension $\gamma_2 = 4 \cdot 10^{-3} \text{ Nm}^{-1}$ (bulk value $\gamma_2 = 12 \cdot 10^{-3} \text{ Nm}^{-1}$). Lower values of the surface tension for thin liquid films in comparison to the corresponding bulk values have been found frequently [2]. However, it is apparent from the Fig. 4 that the harmonic approximation fails to describe our data at film thickness below 15 Å where the measured surface roughness is found to be significantly lower than the theoretical prediction.

A better description of the data can be achieved by using Eqs. (15) and (18) for the surface roughness and film thickness. Note that these expressions influence both the adsorption isotherm and the surface roughness. The best combined refinement for the surface roughness (solid line in Fig. 4) and the adsorption isotherm (almost identical to the previous refinement in Fig. 3) is obtained with the same surface tension $\gamma_2 = 4 \cdot 10^{-3} \text{ Nm}^{-1}$ as before, but now the Hamaker constant is decreased to a value of $A_{\text{eff}} = -7.5 \cdot 10^{-20} \text{ J}$. The parameter D used in Eq. (18) has been found to be a factor of 3 lower than expected from the effective Hamaker constant and the potential given by Eq. (5). It should be noted that our anharmonic approximation is (i) based on a Taylor expansion of the potential terms and (ii) assumes the van der Waals force to be the correct form of the adsorption energy even at molecular coverage. Due to the fact that especially point (ii) is a crude approximation the agreement is surprisingly good.

It has been shown previously that capillary wave fluctuations do have an impact on adsorption isotherms and more realistic potentials than the harmonic approximation are necessary to describe the isotherms properly. While Vorberg *et al.* [12] needed a thickness-dependent surface tension in their self-consistent approach for a thin film on a solid substrate, we can explain our data with a constant surface tension. However, it seems to be a common feature of thin liquid films that their surface tension is lower than the corresponding bulk value.

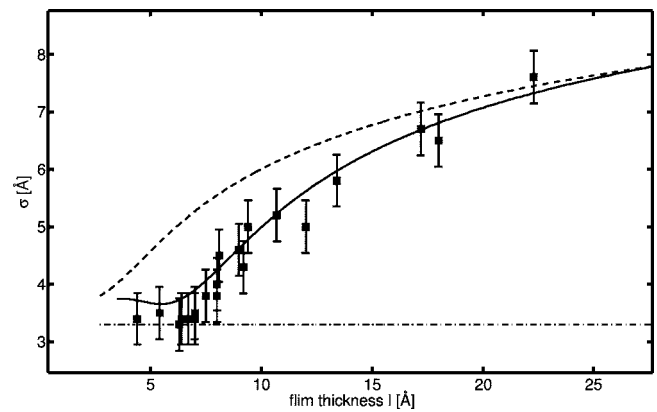


FIG. 4. Measured surface roughness σ_2 as a function of film thickness l . The dashed-dotted line represents the theoretical surface roughness of the glycerol substrate according to Eq. (11). The dashed line is the predicted surface roughness of the thin liquid film within the harmonic approximation given by Eq. (12) (fit with a surface tension $\gamma_2 = 4 \cdot 10^{-3} \text{ Nm}^{-1}$ and $A_{\text{eff}} = -9 \cdot 10^{-20} \text{ J}$). The solid line is the calculation based on the anharmonic approximation [Eq. 22] (fit with a surface tension $\gamma_2 = 4 \cdot 10^{-3} \text{ Nm}^{-1}$ and $A_{\text{eff}} = 7.5 \cdot 10^{-20} \text{ J}$).

V. SUMMARY

In summary, we have measured the adsorption of gas molecules on a liquid surface. We found that molecularly thin layers form on the substrate, with an electron density identical to the value of the corresponding bulk liquid. The measurements yield simultaneous information about the adsorption isotherm and the capillary wave roughness. We find that the harmonic approximation of the interface potential fails to describe the data and higher order terms of the potential are needed to account for a quenching of capillary waves for molecularly thin films. An anharmonic approximation is able to explain our experiments. Explicit expressions for the surface roughness and film thickness as a function of the first higher order potential terms were derived. Even though our approach is a considerable simplification of the real situation, the good agreement between data and theory leads to the conclusion that the model includes the basic features of fluctuations of molecularly thin films.

ACKNOWLEDGMENT

We thank the German Science Foundation (DFG) for financial support (DFG projects GU 535/2-1 and GRK 298).

APPENDIX: THE ANHARMONIC CONTRIBUTIONS TO THE CAPILLARY WAVE ROUGHNESS

In this Appendix we will give a brief outline of our calculations for the anharmonic contributions to the capillary wave roughness. The calculation is based on the formalism of functional calculation. For a detailed treatment see the book of Zinn-Justin [23] and for its application to capillary waves see the paper of Li *et al.* [7]. The change of energy caused by a small perturbation of the surface of a thin film is given by

$$\Delta E = \frac{1}{2} \int d^2r \left\{ \gamma |\nabla h(r)|^2 + \left. \frac{\partial^2 \Omega}{\partial l^2} \right|_{l_m} h(r)^2 + \frac{1}{3} \left. \frac{\partial^3 \Omega}{\partial l^3} \right|_{l_m} h(r)^3 + \frac{1}{12} \left. \frac{\partial^4 \Omega}{\partial l^4} \right|_{l_m} h(r)^4 + \dots \right\}, \quad (\text{A1})$$

where Ω is the interfacial potential. By neglecting all terms of order larger than 2 we obtain the usual expression for capillary waves in the harmonic approximation.

Li and Schlossman [7] used the method of functional integral calculation to treat the higher order terms in the potential as small perturbations. Referring to the book of Zinn-Justin (p. 94) [23] the correlation function can be obtained via the following formalism. A partition function is defined via

$$Z = \int [dh] \exp(-b\Delta E(h)). \quad (\text{A2})$$

with $b = 1/k_B T$. It can be shown that the correlation function is given by

$$\langle h(r_1)h(r_2) \rangle = Z^{-1}(J=0) \left[\frac{\delta}{\delta J(r_1)} \frac{\delta}{\delta J(r_2)} Z(J) \right] \Big|_{J=0} \quad (\text{A3})$$

with

$$Z(J) = \exp\left(-bV_I\left(\frac{\delta}{\delta J(x)}\right)\right) \exp\left(\frac{1}{2}J\Delta J\right), \quad (\text{A4})$$

where V_I denotes the higher order polynomial terms of the potential, i.e.,

$$\begin{aligned} V_I(h) &= \int d^2r \left(\frac{1}{3} \left. \frac{\partial^3 \Omega}{\partial l^3} \right|_{l_m} h(r)^3 + \frac{1}{12} \left. \frac{\partial^4 \Omega}{\partial l^4} \right|_{l_m} h(r)^4 \right) \\ &= \int d^2r (Ch(r)^3 + Dh(r)^4). \end{aligned} \quad (\text{A5})$$

The term $J\Delta J$ is defined as

$$J\Delta J = \int d^2u \int d^2v J(u)\Delta(u,v)J(v) \quad (\text{A6})$$

with the propagator

$$\Delta(x,y) = \frac{1}{b(2\pi)^2} \int d^2q \frac{\exp(iq(x-y))}{\gamma q^2 + m^2} \quad (\text{A7})$$

where m denotes the prefactor of the harmonic term, in our case $m^2 = (\partial^2 \Omega / \partial l^2)|_{l_m}$. Now the exponential in Eq. (A4) is expanded:

$$\begin{aligned} &\exp\left(-b \int d^2r \left(C \left(\frac{\delta}{\delta J(r)} \right)^3 + D \left(\frac{\delta}{\delta J(r)} \right)^4 \right)\right) \\ &\approx 1 - b \int d^2r \left(C \left(\frac{\delta}{\delta J(r)} \right)^3 + D \left(\frac{\delta}{\delta J(r)} \right)^4 \right), \end{aligned} \quad (\text{A8})$$

which allows one to calculate $Z(J)$ and thus the correlation functions.

The third order term C does contribute to the expectation value $\langle h \rangle$, but it cancels out in the calculation of the height-height correlation function and therefore we have to consider the 4th order term only in the following calculation. The partition function reads

$$\begin{aligned} Z(J) &= \left(1 - bD \int d^2r [3\Delta(r,r)\Delta(r,r) + \frac{3}{2}\Delta(r,r)(\Delta J + J\Delta)^2 + \frac{1}{16}(\Delta J + J\Delta)^4] \right) \exp\left(\frac{1}{2}J\Delta J\right). \end{aligned} \quad (\text{A9})$$

The calculation of the correlation function is straightforward but tedious and we only give the final result

$$\begin{aligned} \langle h(r_1)h(r_2) \rangle &= \left(\Delta(r_1, r_2) - 12bD \int d^2r \Delta(0,0)\Delta(r_2, r)\Delta(r_1, r) \right). \end{aligned} \quad (\text{A10})$$

The correlation function evaluated at $r=0$ yields the surface roughness

$$\langle h(0)h(0) \rangle = \sigma^2 \left(1 - \frac{3D}{\pi b \gamma} \left(\frac{1}{m^2} - \frac{1}{(m^2 + q_{uc}^2 \gamma)} \right) \right). \quad (\text{A11})$$

The height-height correlation function can be expressed in an analytical form as

$$\begin{aligned} \langle h(0)h(R) \rangle &= \frac{k_B T}{2\pi \gamma} K_0(R\sqrt{m^2/\gamma}) \\ &\quad - \frac{12D\sigma^2}{4\pi^2 b} \frac{\pi}{\gamma^2} \frac{R}{\sqrt{m^2/\gamma} \Gamma(2)} K_1(R\sqrt{m^2/\gamma}) \end{aligned} \quad (\text{A12})$$

where Γ is the gamma function.

- [1] R. K. Heilmann, M. Fukuto, and P. S. Pershan, Phys. Rev. B **63**, 205405 (2001).
 [2] A. K. Doerr, M. Tolan, W. Prange, J.-P. Schlomka, T. Seydel, W. Press, D. Smilgies, and B. Struth, Phys. Rev. Lett. **83**, 3470

(1999).

- [3] A. K. Doerr, M. Tolan, T. Seydel, and W. Press, Physica B **248**, 263 (1998).

- [4] M. Tolan, X-ray scattering from Soft Matter Thin Films,

- Springer Tracts in Modern Physics, Vol. 148 (Springer, Berlin, 1999).
- [5] K. Mecke, *J. Phys.: Condens. Matter* **13**, 4615 (2001).
- [6] K. R. Mecke, T. Cahritat, and F. Graner, *Langmuir* **19**, 2080 (2003).
- [7] M. Li and M. L. Schlossman, *Phys. Rev. E* **65**, 061608 (2002).
- [8] G. D. Halsey, *J. Chem. Phys.* **16**, 931 (1948).
- [9] T. L. Hill, *J. Chem. Phys.* **17**, 590 (1949).
- [10] J. Frenkel, *Kinetic Theory of Liquids* (Oxford University Press, New York, 1946).
- [11] K. R. Mecke and J. Krim, *Phys. Rev. B* **53**, 2073 (1996).
- [12] J. Vorberg, S. Herminghaus, and K. Mecke, *Phys. Rev. Lett.* **87**, 196105 (2001).
- [13] S. K. Sinha, E. B. Sirota, S. Garoff, and H. B. Stanley, *Phys. Rev. B* **38**, 2297 (1988).
- [14] A. Braslau, P. S. Pershan, G. Swislow, B. M. Ocko, and J. Als-Nielsen, *Phys. Rev. A* **38**, 2457 (1988).
- [15] M. K. Sanyal, S. K. Sinha, K. G. Huang, and B. M. Ocko, *Phys. Rev. Lett.* **66**, 628 (1991).
- [16] M. Li, A. M. Tikhonov, D. J. Chaiko, and M. L. Schlossman, *Phys. Rev. Lett.* **86**, 5934 (2001).
- [17] J. Adin Mann, P. D. Crouser, and W. V. Meyer, *Appl. Opt.* **40**, 4092 (2001).
- [18] B. M. Ocko, X. Z. Wu, E. B. Sirota, S. K. Sinha, and M. Deutsch, *Phys. Rev. Lett.* **72**, 242 (1994).
- [19] M. O. Robbins, D. Andelman, and J. F. Joanny, *Phys. Rev. A* **43**, 4344 (1991).
- [20] A calculation of the expectation value $\langle e^{iq_z(u(r)-u(0))} \rangle$ analogue to [7] shows that we can make use of the expression $\langle e^{iq_z(u(r)-u(0))} \rangle \approx e^{(-2q_z^2(\langle u(0) \rangle^2 + \langle u(0)u(R) \rangle))}$ although u_2 is in principle non-Gaussian. So the surface roughness from Eq. (A4) can be used with Eq. (3).
- [21] T. Seydel, A. Madsen, M. Sprung, M. Tolan, G. Grübel, and W. Press, *Rev. Sci. Instrum.* **74**, 4033 (2003).
- [22] S. Streit, M. Sprung, C. Gutt, and M. Tolan, *Physica B* **357**, 110 (2005).
- [23] J. Zinn-Justin, *Quantum Field Theory and Critical Phenomena* (Clarendon, Oxford, 1989).